Vacuum referred binding energies of the lanthanides in chloride, bromide, and iodide compounds

Dorenbos, Pieter; Josef, Aday; de Haas, Johan; Kramer, Karl W.

DOI
10.1016/j.jlumin.2019.01.009

Publication date
2019

Document Version
Final published version

Published in
Journal of Luminescence

Citation (APA)
Dorenbos, P., Josef, A., de Haas, J., & Kramer, K. W. (2019). Vacuum referred binding energies of the lanthanides in chloride, bromide, and iodide compounds. *Journal of Luminescence*, *208*, 463-467. https://doi.org/10.1016/j.jlumin.2019.01.009

Journal of Luminescence 208 (2019) 463–467

Contents lists available at ScienceDirect

Journal of Luminescence

journal homepage: www.elsevier.com/locate/jlumin

Vacuum referred binding energies of the lanthanides in chloride, bromide, and iodide compounds

Pieter Dorenbos[a,*], Aday Josef[a], Johan T.M. de Haas[a], Karl W. Krämer[b]

[a] Delft University of Technology, Faculty of Applied Sciences, Department of Radiation Science and Technology, Section Luminescence Materials, Mekelweg 15, 2629 JB Delft, Netherlands

[b] Bern University, Freiestrasse 3, CH-3012 Bern, Switzerland

ABSTRACT

A study on Er^{3+} and Yb^{3+} luminescence excitation in $Cs_3Y_2I_9$, Cs_2NaYBr_6, $Cs_3Lu_2Br_9$, YCl_3, YBr_3, and YI_3 is presented. The focus is on determining the energy of the charge transfer band, i.e., the energy needed to transfer an electron from the halide anion (Cl, Br, I) to either Yb^{3+} or Er^{3+}. Those energies together with published spectroscopic information on other lanthanides in the compounds are used to construct vacuum referred binding energies (VRBE) schemes by employing the chemical shift model. Also, VRBE schemes of seven other halide compounds are constructed based on available spectroscopic data. The systematics in the binding energy at the valence band top and conduction band bottom of the thirteen compounds with changing type of halide and with changing compound composition is discussed.

1. Introduction

The Ce^{3+} and Eu^{2+} doped chloride, bromide, and iodide compounds, herein referred to as the halides, form an important family of compounds for application as scintillation detection crystal. $LaCl_3$:Ce^{3+}, $LaBr_3$:Ce^{3+}, Cs_2LiYCl_6:Ce^{3+}, $Cs_2LiLaBr_6$:Ce^{3+}, SrI_2:Eu^{2+} and others are among the best in terms of scintillation light yield, scintillation speed, and energy resolution for gamma photon detection. The 1140 nmnm 4f-4f emission in Tm^{2+} doped $CaCl_2$ and NaCl and other alkali halides are of current interest as solar energy conversion phosphor [1].

The preferred valence of a lanthanide and luminescence quantum efficiency are strongly related with the electronic structure, i.e., the location of the ground and excited states of the lanthanide with respect to the host valence and conduction bands. Fig. 1 shows as typical example the vacuum referred binding energy scheme for the lanthanides in SrI_2 as constructed in [2] by using the chemical shift model from [3]. The level energies and the host band energies are defined as the minimal energies needed to excite an electron from such state or band into the vacuum outside the materials. It requires for example about 4.7 eV to create a photo-electron in the vacuum from the ground state of Ce^{3+}, and the bottom of the conduction band (CB) is here at + 0.37 eV suggesting that SrI_2 is a negative electron affinity material.

The key parameter in the chemical shift model is the U-value for Eu. It is equal to the energy difference between the Eu^{2+} and Eu^{3+} ground states. When known, its value can be used to determine the VRBE in those ground states, and once those are known the VRBEs in each other lanthanide too. The U-value can be derived from the centroid shift of the Ce^{3+} 5d-levels. A compilation of centroid shift values for 150 different compounds that includes 30 different halides can be found in [4]. The U-value for oxide compounds ranges from 6.3 to 7.4 eV, but the range in halide compounds is much narrower. It appears to range from 6.6 to 6.8 eV for chlorides, 6.5–6.6 eV for bromides, and 6.2–6.4 eV for iodides. Generally, for fixed anion type compounds, the U-value tends to increase slightly with higher average electronegativity of the cations in the compounds, it also tends to increase with the size of the site occupied. From the small range and the known trends, always a quite reasonable guess of the U-value can be made. In the case of SrI_2 a value of 6.25 eV was used.

To determine the VRBE E_V at the valence band (VB)-top and/or CB-bottom one needs information on the energy of electron transfer between a lanthanide and a host band. It can e.g. be obtained from optical spectroscopy, thermal quenching of 5d-4f emission in Eu^{2+} or Ce^{3+}, or thermoluminescence glow peak analysis in cases when a lanthanide releases a trapped electron or a trapped hole [5]. For SrI_2 the energy for electron transfer from the VB to Er^{3+} and Nd^{3+} provided the data to establish the VB-top near − 5.3 eV. By adding the energy $E^{ex} = 5.47$ eV of host exciton creation, the VRBE of the electron in the exciton is obtained. In order to arrive at the CB-bottom (E_C) we have to add the exciton binding energy which will be estimated as $0.008 \times (E^{ex})^2$ as proposed in [5]. To test for consistency of the VRBE diagram one may add information on the thermal quenching of Eu^{2+} 5d-4 f emission. In Fig. 1 the lowest 5d-level of Eu^{2+} is found about 1.1 eV below the CB-bottom which is consistent with the very high thermal quenching

* Corresponding author.
E-mail address: p.dorenbos@tudelft.nl (P. Dorenbos).

https://doi.org/10.1016/j.jlumin.2019.01.009
Received 3 September 2018; Accepted 7 January 2019
Available online 09 January 2019

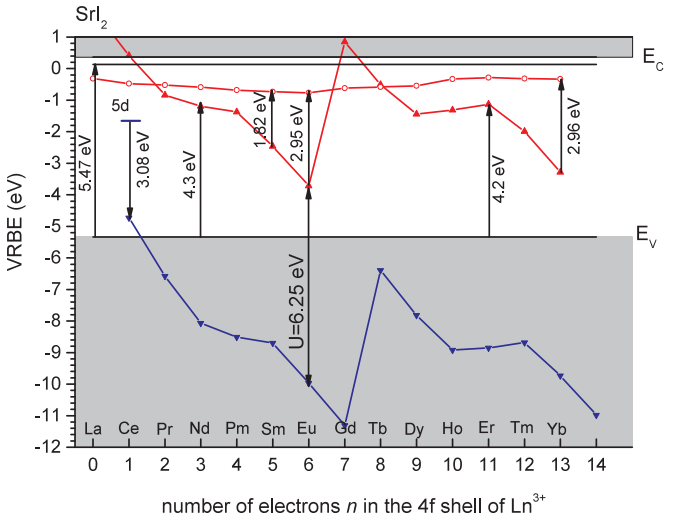

Fig. 1. The VRBE scheme for the lanthanides in SrI_2. The experimentally observed 4f-5d transition energies in Ce^{3+}, Sm^{2+}, Eu^{2+}, and Yb^{2+} are shown together with the Cl → Ln^{3+} charge transfer band energies of Nd^{3+} and Er^{3+} and the host exciton band transition.

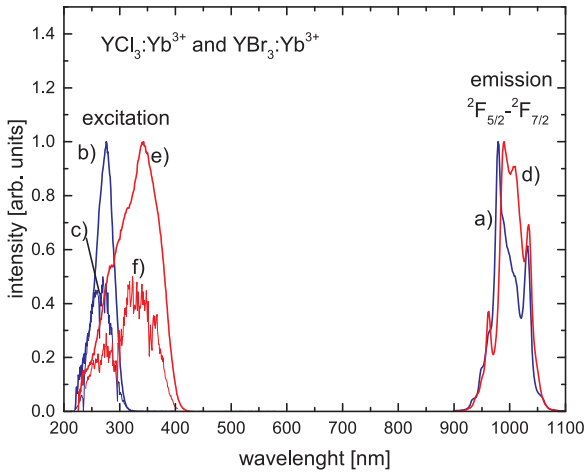

Fig. 2. Curve a) emission of YCl_3:Yb^{3+} under excitation at 276 nm, and b) and c) excitation spectra of 980–990 nm emission. Curve d) emission of YBr_3:Yb^{3+} under excitation at 345 nm, and e) and f) excitation spectra of 1000 nm emission. b) and e) are with Xe-lamp excitation and c) and f) with OPO-laser excitation. All spectra are at room temperature.

temperature that is well above 650 K.

For the halide compounds we have the situation that the U-value can be well-predicted, and there with the VRBE in the ground states of the lanthanides. However, there is still a lack of data that enables to locate the VB-top. For the oxide family of compounds plenty of data is available on the energy of CT to Eu^{3+}, and to much lesser extend to lanthanides like Yb^{3+}, Sm^{3+}, and Tm^{3+}. For the halide compounds Eu^{3+} is usually not the preferred valence but instead that of Eu^{2+}. Then to establish the VB-top one needs to determine the energy of CT to another lanthanide than Eu^{3+}.

In this work we studied $Cs_3Y_2I_9$:1% Er^{3+}, Cs_2NaYBr_6:10%Yb^{3+}, $Cs_3Lu_2Br_9$:5% Yb^{3+}, YCl_3:1% Yb^{3+}, YBr_3:1%Yb^{3+}, YI_3:1% Er^{3+} with the aim to determine the energy of the VB → Ln^{3+} charge transfer (CT). In addition we collected data available in literature on lanthanide spectroscopy in seven other halide compounds. Altogether sufficient information is gathered to construct VRBE schemes for thirteen different halide compounds from which trends and systematics in the location of the VB-top and CB-bottom can be derived. Those trends and systematics can serve as future reference or benchmark to construct, or make educated guesses for, VRBE schemes of other halide systems.

2. Results

The materials of study are fragments of transparent single crystals with typical sizes of 4 × 4 × 2 mm^3 that originate from larger single crystal boules grown with the vertical Bridgman technique. The binary starting materials were sealed in silica ampoules under vacuum, heated above the melting point, and slowly cooled by moving the furnace with 0.01 mm/minute during crystallization. Rare earth chlorides and bromides were prepared according to the ammonium halide method from oxides of 5N-6N purity. Rare Earth iodides were synthesized from the elements of 3N-4N purity in evacuated silica ampoules. All rare earth halides were sublimed in vacuum for further purification. Alkali halides were dried in vacuum at 300 °C. The materials were grown from stoichiometric melts except for $Cs_3Lu_2Br_9$:5% Yb^{3+} which melts incongruently. It was grown from a 55 mol% CsBr and 45 mol% $REBr_3$ melt. All handling was done under strictly dry conditions in a closed apparatus or glove box.

For the luminescence excitation and emission studies we used in house facilities. Excitation was performed either by a Xe-lamp or by an OPO pulsed laser system at room temperature (RT) or 10–20 K. Presented excitation spectra were corrected for the excitation intensity. Due to fluctuating pulse intensity and position focus of the OPO pulses, the correction is somewhat poor. However since we are interested in determining the energy of rather wide charge transfer bands, a poor correction does not much affect our results.

Fig. 2 shows the RT excitation of 980 nm Yb^{3+} 4f-4f emission together with the emission under excitation at 276 nm (4.49 eV) for YCl_3 and 345 nm (3.59 eV) for YBr_3. For both compounds the emission is from the $^2F_{5/2} \rightarrow ^2F_{7/2}$ transitions in Yb^{3+}. The Yb^{3+} CT-band is observed at 276 nm with FWHM of 38 nm (0.61 eV). With OPO-laser excitation (spectrum c) the excitation maximum is near 271 nm, and therefore the RT CT-band energy is evaluated at 4.53 eV. For YBr_3 the maximum of the CT band shifts towards 341 nm (Xe-lamp excitation and 331 nm OPO-laser excitation). The CT-band energy is evaluated at 3.69 eV with FWHM of 0.8 eV. The CT-energies for YCl_3 and YBr_3 are quite similar to the values of 37900 cm^{-1} (4.59 eV) and 28200 cm^{-1} (3.50 eV) reported by Barnes and Pincott in 1966 [6] for $YbCl_3$ and $YbBr_3$. The in crystal ionic radii for Y^{3+} (104 pm) and Yb^{3+} (116 pm) are not too much different and both compounds adopt closely related $AlCl_3$ and BiI_3 type structures, respectively. Apparently one may regard the pure Yb-compound as a Y-compound with 100% Yb^{3+}. We did not observe any charge transfer luminescence from Yb^{3+} at room temperature.

Fig. 3 shows the excitation spectra of Yb^{3+} in Cs_2NaYBr_6 with an elpasolite crystal structure, and in the ternary compound $Cs_3Lu_2Br_9$ with a $Cs_3Tl_2Cl_9$ type structure. Both compounds exhibit (distorted) octahedral Yb^{3+} coordination like the MX_3 compounds above. The Yb^{3+} CT-band appears in both compounds around 365 nm (3.40 eV) with 0.81 eV and 0.63 eV (FWHM based on the OPO-laser excitation spectra) for Cs_2NaYBr_6 and $Cs_3Lu_2Br_9$.

YI_3 with Ce^{3+} was studied by Srivastava et al. [7], and based on that work the Ce^{3+} 5d centroid shift could be determined from which a U-value of 6.29 eV was derived in [4] which is similar to that for SrI_2. The excitation of the Er^{3+} $^4S_{3/2} \rightarrow ^4I_{15/2}$ 4f-4f emission at 553 nm in Fig. 4 shows at room temperature a broad band peaking at 336 nm with a short wavelength shoulder around 310 nm, and with Er^{3+} excitation lines between 350 and 450 nm. The X-ray excited emission at RT shows the characteristic Er^{3+} lines in spectrum b). At 17 K, the excitation spectrum of 553 nm Er^{3+} emission is different. The above short wavelength shoulder develops into the dominant band and the 336 nm band is now present as a relatively weak long wavelength shoulder band, see spectrum c). In addition, a relatively sharp excitation band develops at 281 nm. Srivastava et al. observed similar 310 nm

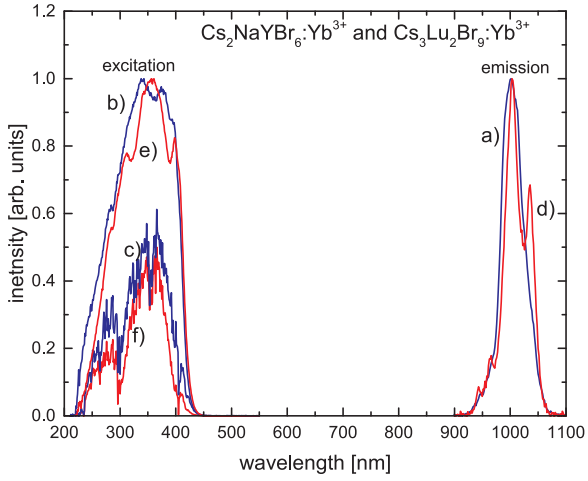

Fig. 3. Curve a) emission of $Cs_2NaYBr_6:Yb^{3+}$ under excitation at 365 nm, and b) and c) excitation spectra of 995 nm emission. Curve d) emission of $Cs_3Lu_2Br_9:Yb^{3+}$ under excitation at 340 nm, and e) and f) excitation spectra of 980–990 nm emission. b) and e) are with Xe-lamp excitation and c) and f) with OPO-laser excitation. All spectra are at room temperature.

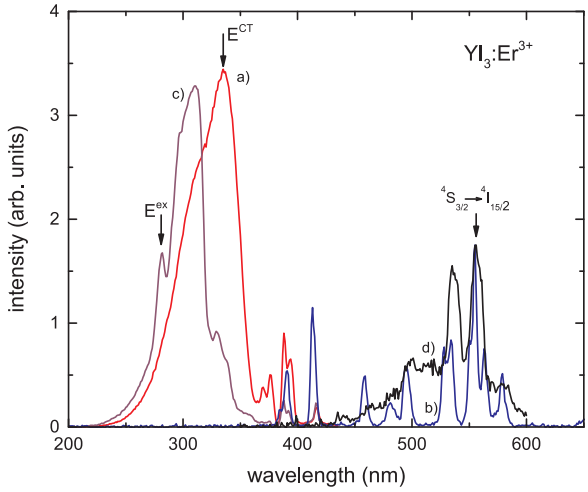

Fig. 4. Excitation and emission spectra of $YI_3:Er^{3+}$. a) the room temperature Xe-lamp excitation spectrum of $^4S_{3/2} \rightarrow ^4I_{15/2}$ Er^{3+} emission at 553 nm, b) X-ray excited emission at RT, c) the 17 K Xe-lamp excitation spectrum of Er^{3+} emission at 553 nm, d) 17 K emission excited at 310 nm.

excitation band in the excitation spectrum of Ce^{3+} at 80 K, and it therefore seems to be related to the YI_3 host material and not to the dopants. Under excitation at 310 nm a broad band emission appears between 450 and 600 nm underneath the Er^{3+} emission, see spectrum d) in Fig. 4 which is absent at RT. We attribute the excitation band near 332 nm (3.73 eV) to the iodine to Er^{3+} charge transfer band. The excitation band around 310 nm with the broad emission between 450 and 600 nm cannot be the host exciton because the fundamental absorption of the YI_3 host is reported at shorter wavelength of 300 nm [7]. It is therefore attributed to unknown defect excitation and emission in YI_3. The relatively sharp band at 280 nm (4.43 eV) for Er^{3+} doping is seen as a 277 nm (4.48 eV) shoulder band for Ce^{3+} doping in [7], and we attribute it in this work to the host exciton creation band.

$Cs_3Y_2I_9$ doped with Er^{3+} was studied by Luthi et al. [8]. It has a $Cs_3Cr_2Cl_9$ type structure closely related to $Cs_3Lu_2Br_9$. They observed at 10 K an absorption band at 337 nm (3.68 eV) with about 0.25 eV FWHM followed by a steep rise at 322 nm (3.84 eV) attributed to the fundamental absorption onset. From the typical Ce^{3+} 4f-5d absorption energy of 3 eV in iodides, that for Er^{3+} is expected well above 6 eV. The

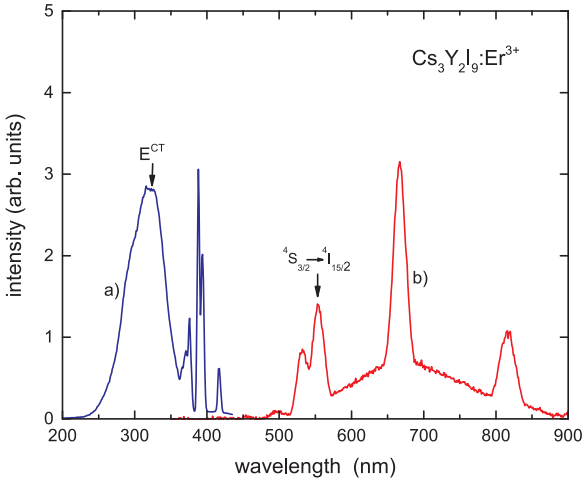

Fig. 5. a) The excitation spectrum of 550 nm $^4S_{3/2} \rightarrow ^4I_{15/2}$ Er^{3+} emission and, b) emission excited at 315 nm in $Cs_3Y_2I_9$ at RT.

3.68 eV absorption can therefore not be attributed to a 4f-5d transition as suggested in [8]. In our study at RT we observe when monitoring 550 nm emission a broad excitation band between 275 nm and 350 nm with maximum around 325 nm, see spectrum a) in Fig. 5. Excitation at 315 nm yields Er^{3+} 4-4f emission lines together with a broad band emission, see spectrum b) in YI_3 in Fig. 4. The excitation spectrum a) for $Cs_3Y_2I_9$ is quite similar as spectrum a) for YI_3 in Fig. 4. Based on our work and in [8] we estimate the CT-band at 330 nm (3.76 eV).

3. Discussion

The aim of this work is to arrive at a collection of VRBE schemes for the lanthanides in halide compounds that can act as a benchmark for other compounds within this family. Table 1 compiles the data on Er^{3+} and Yb^{3+} CT-band energies of the six compounds studied in this work. We have added data on $LaCl_3$, Cs_2NaYCl_6, $LaBr_3$, SrI_2, $CsMgI_3$, LaI_3, and LuI_3. The U-parameters for many of the compounds were derived in [4] from Ce^{3+} centroid shift data. For the other compounds estimates were made taking into account that U tends to reduce with smaller value for the electronegativity of the cations in the compound. It also tends to reduce with smaller site size. VRBE data and schemes for $LaCl_3$, $LaBr_3$, and LaI_3 were already presented in [9,4] and for SrI_2 in [2]. For each of the compounds in Table 1, a brief account on how data were obtained or estimated is presented in the Appendix.

Table 1 compiles the relevant parameters needed to construct VRBE schemes like for SrI_2 in Fig. 1. The exciton creation energy E^{ex} usually increases slightly (few 0.1 eV) when temperature is lowered from RT to

Table 1
The parameter values in eV needed to construct VRBE diagrams. Values listed in italic font are tentative or estimated values.

A	E^{ex}	$E^{CT}(Ln^{3+})$	$E^{CT}(Eu^{3+})$	U	$D(3+)$	E_V
$LaCl_3$	6.5	4.49 (Sm); 5.28 (Dy)	3.12	6.8	1.63	− 7.09
YCl_3	*7.0*	4.53 (Yb)	4.10	6.70	2.42	− 8.02
Cs_2NaYCl_6	7.25	5.44 (Sm); 6.74 (Er); 5.96 (Tm)	4.20	6.67	2.55	− 8.11
$LaBr_3$	5.40	4.96 (Pr); 4.38 (Er)	1.90	6.60	2.09	− 5.77
YBr_3	*6.9*	3.69 (Yb)	3.26	6.53	*2.9*	− 7.10
Cs_2NaYBr_6	6.16	3.40 (Yb)	2.96	6.53	2.76	− 6.80
$Cs_3Lu_2Br_9$	*5.85*	5.46 (Er); 3.40 (Yb)	2.96	6.55	2.72	− 6.81
SrI_2	5.47	4.3 (Nd); 4.2 (Er)	1.63	6.25	*2.84*	− 5.34
$CsMgI_3$	4.84	4.04 (Dy); 4.21 (Er)	1.7	6.25	–	− 5.41
LaI_3	3.4	–	*1.30*	6.30	3.19	− 5.04
YI_3	4.45	3.73 (Er)	1.15	6.29	3.10	− 4.88
$Cs_3Y_2I_9$	*4.45*	3.76 (Er)	1.18	6.25	–	− 4.89
LuI_3	4.30	3.97 (Pr)	1.10	6.22	3.15	− 4.80

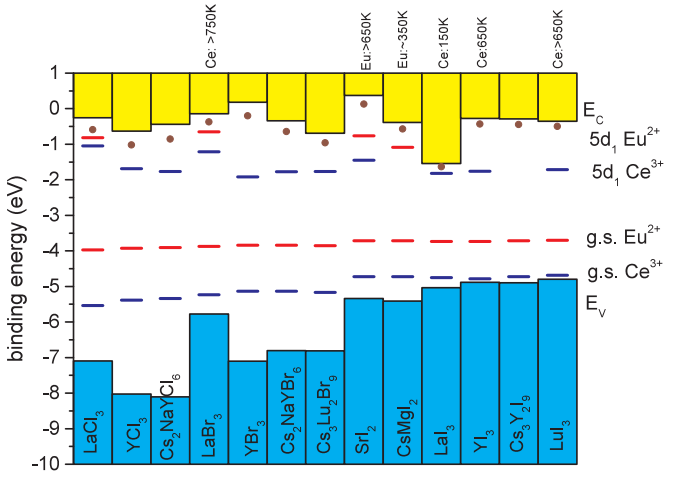

Fig. 6. The stacked VRBE schemes of the halide compound. Horizontal levels denote the VRBE in the ground state of Ce^{3+} and Eu^{2+}, and the lowest energy 5d state of Ce^{3+} and Eu^{2+}. The bullet points are the VRBE of the electron in the host exciton state. The end and starts points of the vertical bars indicated the energy at the top of the VB and bottom of the CB. If available, the temperature $T_{50\%}$ for 5d-4f emission is given.

10 K. For best comparison of different compounds with each other, E^{ex} refers to the measured values at ≈ 10 K and otherwise the RT value augmented by 0.1–0.15 eV is listed. The U-value in column 5 provides, by employing the chemical shift model, the VRBE energies in the divalent and trivalent lanthanide ground states as connected by the zigzag curves in Fig. 1. Column 3 lists the CT data for Yb^{3+} and Er^{3+} as found in this work, and CT-data from literature sources (see Appendix). Since there is always a constant energy difference between the CT to a lanthanide and the CT to Eu^{3+}, one may derive that for Eu^{3+} as listed in column 4. The value for LaI_3 is in italics because no CT-data is available, and the method outlined in the Appendix was used instead to estimate its value. The redshift $D(3+)$ in column 6 is from compiled Ce^{3+} $4f-5d_1$ excitation band energies in [4] and is used to determine the VRBE in the lowest Ce^{3+} 5d-level. E_V in the last column is the VRBE at the top of the valence band as obtained by applying the chemical shift model on the data. By adding $E^{ex}\times(1+0.008\,E^{ex})$ the energy E_C at the CB-bottom is reached.

To illustrate how band and level energies change with type of compound, the data from Table 1 were used to construct the stacked VRBE scheme of Fig. 6. The Eu^{2+} ground state is, as usual, always near − 4 eV. It rises from − 4.0 eV to − 3.7 eV when the U-value becomes smaller in going from a chloride to a bromide to an iodide compound. Within the chemical shift model this is caused by the increasingly weaker bonding of the anion ligands enabling a better screening of the Eu^{2+} cationic charge, i.e., the anion electrons can move closer towards the lanthanide. The closer proximity of the negative screening charge provides increased Coulomb repulsion with the 4f-electrons. It decreases the 4f-electron binding and thus raising (becomes less negative) the VRBE. The same applies for Ce^{3+}, but since the total screening charge is 3- instead of 2-, and since Ce^{3+} is smaller than Eu^{2+}, the raising effect on the VRBE is more than a factor 1.5 stronger. The VRBE in the lowest 5d level of Ce^{3+} is always found around -1.8 ± 1 eV. The variations therein are caused by the size of the crystal field splitting of the 5d-levels [10]. $LaCl_3$ and $LaBr_3$ share the same crystal structure, and Ce^{3+} is 9-fold coordinated with a tri-caped trigonal prism of anions. Such coordination leads to very small (<1 eV) crystal field splitting [11,12], and consequently the 5d level is at relatively high VRBE in Fig. 6. Except for SrI_2 all other compounds have 6-fold (distorted) octahedral coordination with much larger (2–3 eV) crystal field splitting. In the stacked VRBE diagram this translates to a 0.4–0.5 eV lower location of the 5d-level. The 5d-level of divalent lanthanides like Eu^{2+} is always 0.5–1.0 eV above that of Ce^{3+} simply because the 5d electron is less strongly bonded to the lower charged Eu^{2+}.

The 50% luminescence thermal quenching temperature T_{50} of Eu^{2+} and Ce^{3+} 5d-4f emission relates to the energy difference ΔE between the emitting 5d-level and the conduction band bottom as [13]

$$\Delta E = k_B \ln\left(\frac{\Gamma_0}{\Gamma_\nu}\right) T_{50} \quad (1)$$

With typical values of $\Gamma_0 = 3\times10^{13}$ Hz for the vibrational frequency, and radiative rates $\Gamma_\nu = 2\times10^6$ Hz for Eu^{2+} and 3×10^7 Hz for Ce^{3+} one obtains a variation in T_{50} of ≈ 700 K/eV for Eu^{2+} and of ≈ 840 K/eV for Ce^{3+}.

The stacked scheme shows that both the VRBE in the 5d-level and the VRBE at the CB-bottom changes with type of compound which makes a beforehand prediction of thermal quenching temperature complicated. Even when the VRBE diagram is well-established still the quenching barrier ΔE is not well-defined because of lattice relaxation and related Stokes shift that will alter level locations. Anyway, a clear correlation between known quenching temperatures for Ce^{3+} and Eu^{2+} 5d-4f emission as listed at the top of the stacked diagram with ΔE from the VRBE scheme is observed. Quenching of Eu^{2+} emission in $CsMgI_3$ is for example at more than 300 K lower temperature than in SrI_2 which is mainly caused by a lower VRBE at the CB-bottom.

A basic understanding on the VRBE in the lowest energy 5d-state is available, but that at the CB-bottom is still lacking because information on CB VRBE values was never available. Based on stacked diagrams as in Fig. 6, a first assessment can be made. The VRBE at the bottom of the conduction band is determined by the binding energy of an electron that resides in the orbitals formed by the cations. Apart from SrI_2 and $CsMgI_3$, the compounds in Fig. 6 are trivalent rare earth based compounds and the bottom of the conduction band is dominated by 5d-orbitals (La, Lu) or 4d-orbitals (Y). This means that as first approximation the CB-bottom of an Ln^{3+} based compound is at energies comparable to that of the 5d-electron in a divalent lanthanide dopant like Eu^{2+}. Indeed, the Eu^{2+} 5d-level is either close to the CB-bottom but usually inside the CB in trivalent rare earth based compounds [14].

The VRBE at the top of the valence band is foremost determined by the type of anion. In [15] VRBE schemes for fluoride compounds were presented and the top of the valence band was found at typical energies of − 12 eV in agreement with known results from photo-electron spectroscopy. Fig. 6 shows that for Cl^- to Br^- to I^- the VRBE at the VB-top increase to typical values of − 8 eV, − 7 eV, and − 5.5 eV.

Summarizing, in this work the energy of charge transfer from the chlorine, bromine, and iodine valence band to Er^{3+} and Yb^{3+} in various halide compounds was determined. By also using spectroscopic data on lanthanides in other compounds, the needed parameters to construct VRBE diagrams for the lanthanides in 13 different compounds were established. The Eu^{2+} ground state energy is the most compound invariant. It is lowest for chlorides (−4 eV for $LaCl_3$) and highest for iodides (−3.7 eV for LaI_3). The VRBE in the lowest 5d-level correlates with the size of the crystal field splitting. The large crystal field splitting for e.g. Ce^{3+} on octahedral sites leads to relatively low lying 5d-levels, and the small crystal field splitting on the 9-fold coordinated sites in $LaCl_3$ and $LaBr_3$ leads to about 0.5 eV higher VRBE. The dominant change in the VRBE diagram is the energy at the top of the VB. it changes from values around − 8 eV, − 7 eV, and − 5.5 eV for chlorides, bromides, and iodides respectively.

Appendix A. Appendix

The experimental data or methods to estimate the values for the parameters needed to construct VRBE diagrams, as listed in Table 1, are provided in this appendix.

For $LaCl_3$, we use a slightly revised value of 3.12 eV for the estimated Eu^{3+} CT-band energy. It is obtained from the observed Sm^{3+}

and Dy^{3+} CT-bands at 4.49 eV and 5.28 eV in [16]. For the rest the data is unaltered from [9,4]. For YCl_3 the redshift $D(3+)$ for the trivalent lanthanides is obtained from Ce^{3+} data in [17]. Information on host exciton creation was not found and in Table 1 a tentative value that is 0.5 eV larger than that of $LaCl_3$ is listed. For Cs_2NaYCl_6 sufficient information is available on CT-data, i.e. for Sm^{3+} and Yb^{3+} in [18], and for Tm^{3+} in [19]. Data on the 4f-5d transition can be found for Ce^{3+} in [20,21], for Pr^{3+} in [21,22], and for Tb^{3+} in [23]. E^{ex} is from [18,24,25].

Data for $LaBr_3$ is the same as in [9,4]. For YBr_3 we again entered an estimated value for E^{ex} about 0.5 eV larger than that of $LaBr_3$. The Ce^{3+} 5d-4f emission to the ground state is near 430 nm [26], and assuming a typical Stokes shift of 0.3–0.4 eV the redshift $D(3+)$ is estimate 2.9 eV. All data on Cs_2NaYBr_6 is from [27]. For $Cs_3Lu_2Br_9$, E^{ex} is estimated 5.85 eV; the same as observed for $LuBr_3$ [28]. The redshift $D(3+) = 2.72$ eV is from own work based on unpublished data on Ce^{3+}. The absorption spectrum of Er^{3+} in $Cs_3Lu_2Br_9$, as presented in [8], shows a band starting at 43000 cm^{-1} (5.33 eV) with its maximum beyond the instrumental limit of 43500 cm^{-1}. It was attributed to the 4f-5d transition in Er^{3+}, and with an estimated energy of ≈ 44000 cm^{-1} (≈ 5.46 eV) this corresponds with a redshift $D(3+) = 4.4$ eV. Since this deviates much too far from the value for Ce^{3+}, the assignment cannot be correct. Assigning it to the Er^{3+} CT band is, however, fully consistent with what is predicted from the 3.35 eV Yb^{3+} CT-band energy observed in Fig. 3.

Data for SrI_2 are from [2] where Er^{3+} CT-bands were observed at 295 nm (4.20 eV) and 347 nm (3.47 eV). The high energy band was assigned to the genuine VB → Er^{3+} CT-band, and the low energy band was tentatively attributed to CT from an interstitial charge compensating iodine. Assignment is consistent with the Nd^{3+} CT-band at 4.3 eV from [29]. The redshift for Ce^{3+} is not known, but it can be estimated from the 3.08 eV energy of emission to the ground state from [30]. Assuming a 0.2 eV large Stokes shift, we arrive at $D(3+) \approx 6.12 - 0.2 - 3.08 = 2.84$ eV. E^{ex} and data on CT-band energies for $CsMgI_3$ are from [31], and data for Eu^{2+} from [32]. For LaI_3 no CT-data is available, and we need alternative methods to determine the VRBEs. From the 140 KT_{50} quenching temperature of Ce^{3+} 5d-4f emission in [33] we know that the 5d level must be within a few 0.1 eV from the CB-bottom. A broad band emission around 720 nm (1.72 eV) for Yb^{2+} in LaI_3 has been assigned to anomalous emission by Hendriks and van der Kolk [34]. Upon exciting the lowest 5d state located inside the CB luminescence is from the CT arises from the CB → Yb^{3+} transition. With a value of 1.3 eV estimated for the CT-band energy of Eu^{3+} the most consistent VRBE scheme is obtained. For LuI_3 different parameters than in [9] were used. Here we used the U-value of 6.22 eV from [4], and the Eu^{3+} was estimated from the CT-band to Pr^{3+} observed around 312 nm (3.97 eV) in [35]. The data for YI_3 and $Cs_3Y_2I_9$ were presented in the results section. Tentatively, we assume that the host exciton creation energy for $Cs_3Y_2I_9$ is the same as in YI_3.

References

[1] Otmar M. ten Kate, Karl W. Krämer, Erik van der Kolk, Sol. Energy Mater. Sol. Cells 140 (2015) 115.
[2] Mikhail S. Alekhin, Roy.H.P. Awater, Daniel A. Biner, Karl W. Krämer, Johan T.M. deHaas, Pieter Dorenbos, J. Lumin. 167 (2015) 347.
[3] P. Dorenbos, Phys. Rev. B 85 (2012) 165107.
[4] P. Dorenbos, J. Lumin. 135 (2013) 93.
[5] P. Dorenbos, Opt. Mater. 69 (2017) 8.
[6] J.C. Barnes, H. Pincott, J. Chem. Soc. A (1966) 842.
[7] A.M. Srivastava, S.J. Camardello, H.A. Comanzo, M. Aycibin, U. Happek, Opt. Mat. 32 (2010) 936.
[8] S.R. Lüthi, H.U. Güdel, M.P. Hehlen, J. Chem. Phys. 110 (1999) 12033.
[9] P. Dorenbos, J. Lumin. 136 (2013) 122.
[10] P. Dorenbos, J. Lumin. 169 (2016) 381.
[11] P. Dorenbos, Phys. Rev. B62 (2000) 15650.
[12] P. Dorenbos, J. Alloy. Compd. 341 (2002) 156.
[13] P. Dorenbos, J. Phys. Cond. Matter 17 (2005) 8103.
[14] P. Dorenbos, J. Lumin. 128 (2008) 578.
[15] P. Dorenbos, Phys. Rev. B 87 (2013) 035118.
[16] S.M. Kuzakov, E.F. Martynovich, I.A. Parfianovich, Izv. Akad, Nauk SSSR Ser. Fiz. 41 (1977) 1380.
[17] V.L. Cherginets, T.V. Ponomarenko, L.N. Trefilova, N.V. Rebrova, N.N. Kosinov, V.D. Alekseev, O.V. Zelenskaya, Inorg. Mater. 45 (2009) 946.
[18] P.A. Tanner, C.-K. Duan, B.-M. Cheng, Spectrosc. Lett. 43 (2010) 432.
[19] Chang-Kai Duan, Peter A. Tanner, Andries Meijerink, Vladimir Babin, J. Phys. Cond. Matter 21 (2009) 395501.
[20] R.W. Schwartz, P.N. Schatz, Phys. Rev. B 8 (1973) 3229.
[21] M. Laroche, M. Bettinelli, S. Girard, R. Moncorgé, Chem. Phys. Lett. 311 (1999) 167.
[22] P.A. Tanner, C.S.K. Mak, M.D. Faucher, W.M. Kwok, D.L. Philips, V. Mikhailik, Phys. Rev. B67 (2003) 115102.
[23] L. Ning, C.S.K. Mak, P.A. Tanner, Phys. Rev. B72 (2005) 085127.
[24] P. Putaj, J.T.M. de Haas, K.W. Krämer, P. Dorenbos, IEEE Trans. Nucl. Sci. 57 (2010) 1675.
[25] Guohua Jia, Bing-Ming Cheng, Chang-Kui Duan, P.A. Tanner, Chem. Phys. Lett. 515 (2011) 235.
[26] V.I. Cherginets, T.P. Rebrova, T.V. Ponomarenko, O.A. Tarasenko, N.N. Kosinov, O.V. Zelenskaya, Rad. Meas. 47 (2012) 917.
[27] M.D. Birowosuto, P. Dorenbos, C.W.E. van Eijk, K.W. Krämer, H.U. Güdel, J. Phys. Condens. Matter 18 (2006) 6133.
[28] O. Guillot-Noël, J.T.M. de Haas, P. Dorenbos, C.W.E. van Eijk, K. Krämer, H.U. Güdel, J. Lumin. 85 (1999) 21.
[29] I.N. Ogorodnikov, V.A. Pustovarov, A.A. Goloshumova, L.I. Isaenko, A.P. Yelisseyev, V.M. Pashkov, J. Lumin. 143 (2013) 101.
[30] C.M. Wilson, E.V. van Loef, J. Glodo, N. Cherepy, B. Hull, S. Payne, W.-S. Choong, W. Moses, K.S. Shah, Proc. SPIE 7079 (2008) 707917.
[31] G.L. McPherson, K. Talluto, Solid State Commun. 43 (1982) 331.
[32] M. Suta, C. Wickleder, J. Mater. Chem. C 3 (2015) 5233.
[33] A. Bessiere, P. Dorenbos, C.W.E. van Eijk, K.W. Krämer, H.U. Güdel, Nucl. Instrum. Methods A537 (2005) 22.
[34] Maurice Hendriks, Erik van der Kolk, J. Lumin. 207 (2019) 231 under review.
[35] A.M. Srivastava, Opt. Mater. 30 (2008) 1567.